

Thermal Decomposition Behavior of Sericin Cocoon

MASUHIRO TSUKADA, *Sericultural Experimental Station, Suginami-ku, Tokyo, Japan*

Synopsis

The behavior on thermal degradation of the sericin cocoon consisting of a sericin and a few fibroin has been examined by means of evolved gas analysis (EGA), evolved gas detection (EGD), and differential thermal analysis (DTA). The sericin cocoons produced from the silkworm (Nd, Nd-s/Nd-s, Nd-s/+) and sericin stripped from the silk gland in the silkworm show two endothermic peaks at 220° and 270°C according to differential thermal analysis. From the x-ray diffraction pattern, dynamic mechanical measurement, and the thermal gravity analysis (TG), the former peak occurs by the scission of the structural state and the change from crystalline to amorphous. Moreover, at 220°C, the weight changes markedly, the yellowness index (L/b) measured by the color difference meter abruptly decreases, and the gas (CO_2), evolved from the sericin cocoon, shows increases above 200°C.

INTRODUCTION

From the cross section view of the bave spun by a mature silkworm, it is observed that gumming sericin surrounds the silk brins. These gumming sericins are repeatedly subjected to significant mechanical and thermal forces in the reeling process. Moreover, cocoons are exposed to heat of over 110°C for several hours in the drying chamber. This thermal treatment produces injurious effects such as denaturing of the cocoons; consequently, the reelability of the silk or the raw silk properties from these cocoons may be slightly to markedly changed. This paper deals with the responses of sericin to thermal changes.

There have been previous explanations of the complexity of sericin and the solid-state sericin components. Rutherford and Harris¹ suggest the uniprotein theory of sericin. Shimizu² and Mosher³ support the uniprotein theory and suggest that sericin consists of various protein components, based on the classification of sericin with different solubilities. The pyrolytic behavior of silk treated with Sn-complex has been reported by Koide.⁴ Although Aoki⁵ and Hirabayashi^{6,10} independently investigated the thermal characteristics of the sericin cocoon, a satisfactory explanation for the thermal degradation mechanism has not yet been obtained. For this reason, the author has investigated the fine structures of sericin cocoons in order to compare them with the thermal properties of the sericin extracted from the cocoon and the sericin classified by Mosher and Shimizu.

The sericin cocoon appears equally utilizable as the native liquid sericin sample judging from the results of the electrophoretic patterns¹⁴ of the samples used in this study. In these electrophoretic patterns, the sericin cocoons showed exactly the same pattern as those of the liquid sericin in the sericin silk gland of silkworms. The results of the electrophoretic analysis of the sericin indicate that there are no distinct differences in the molecular weight and the configuration of the sericin cocoons and the liquid sericin in the silk gland of the native

sericin (sericin silkworm), nor are there any distinct differences in their thermal decomposition behavior.

from the chemical, biometric, and x-ray diffraction pattern analysis, the amino acid sequences and structural characters have been partly clarified. But satisfactory explanations for thermal stability of the sericin have not been obtained. As mentioned above, the heating and drying process is often repeated in the filature and silk industry. In this paper, the structural characteristics of the sericin are subjected to analysis by measuring their decomposition behavior. The evolved gas from these samples were analyzed.

EXPERIMENTAL

Materials

Samples characterized by low or absent fibroin action were used in this experiment. These samples are of the variety of the naked pupa mutant which produce cocoons consisting mainly of sericin, and naked pupa such as Nd, Nd-s/Nd-S, Nd-s/+, and Pnd sericin silkworms which do not produce cocoons (see Appendix). The sericin cocoon layer and Hakuri sericin, which is stripped from coagulated silk fibroin, and β -type fibroin, which gives x-ray diffraction patterns of β -structure, were also used. Coagulated fibroin and β -type fibroin were also used to compare their fine structures. These samples were cleaned by solvent (benzene:methanol = 1:1) in a Soxhlet extractor at 95°C for 50 hr to remove wax and pigment, then rinsed in distilled water, dried to constant weight, and conditioned in air at room temperature. The β -type fibroin was obtained by degumming the raw silk using boiling water for 2 hr.

Method

The analysis of evolved gas was carried out with the evolved gas detection instrument (EGD) Model OT-20B, EGA-20-type gas chromatography made by Simazu Seisaku-sho. EGD measurement conditions were as follows: measurement atmosphere, He; measurement sensitivity, 8 mV (100 mA); chart speed, 5 mm/min. Organic gas detection was carried out with a hydrogen ion detector (HID) equipped with gas column PEG-20M which detects hydrocarbons. Chromatograms for gas detection were obtained with Model GC-4BPTF; carrier gas, N₂; inlet pressure, 1.8 kg/cm²; H₂ and air flow rate, 0.5 and 1.0 kg/cm². The inorganic gas chromatogram measurements were obtained with Model GC-6AMPTF; carrier gas, He; inlet pressure, 3 kg/cm²; detector, TCD; bridge current, 170 mA; range, 16 and 1 mV; detector temperature, 150°C; injection temperature, 50°C; chart speed, 5 mm/min. The parallel separation method (Fig. 1) was used to detect and analyze the evolved gas from the sericin. In Figure 1, the tube was Shimalite Q (1.5 m) silica gel (2.0 m); and MS-5A (5 m × 3 mm). Microdifferential thermal analysis was carried out under the following conditions; measurement sensitivity, ±100 mV; heating rate, 10°C/min; measurement atmosphere, He; chart speed, 5 mm/min; measurement atmosphere, He; chart speed, 5 mm/min. The sample (15 mg) was packed in an aluminum pan.

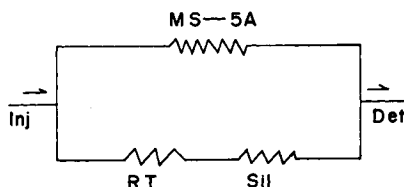


Fig. 1. Schematic diagram of parallel separation system for detection of thermally evolved gas: RT, resistant tube; Sil, silica gel; Inj, injection side; Det, detection side.

RESULTS AND DISCUSSION

Thermal Gravity Analysis and Differential Thermal Analysis

Several sericin cocoons (hereditary notation Nd, Nd-s/Nd-s, Nd-s/+, and Pnd) and sericin which was stripped from coagulated fibroin extracted from fifth-stage mature silkworms (*bombyx mori*) were prepared as samples following removal of the wax substances and pigments. The weights of the samples were measured in relation to time and temperature (TG scan) and were heated from 80° to 400°C. In the TG experiment with these sericin samples, almost all of the sericin had similar features in the weight-temperature profile. The experimental curve for the TG measurement of Nd-s/Nd-s is comparable to that for the typical sericin cocoon (Fig. 2). The weight loss trace indicates that initial weight loss occurred because of the volatilization endotherm of the sericin at the same temperature region (90°C) on the micro-DTA thermograms. The second weight loss can be seen in the wide temperature range from 170° to 300°C; thermal decrease of the weight occurred at 220°C. Then abrupt decrease in weight was detected in the wide temperature range from 220°C upward. At 200°C, though the sericin weight residue is about 90%, the sericin shows gradual decrease in weight until 400°C (Fig. 2). The residue of the weight decreases to 40% at 400°C. The DTA response for sericin cocoon (Nd-s/Nd-s) shows no change from 100° to 210°C, at which point some endothermic reaction (second peak) occurs, and is followed by a third and fourth peak at 270° and 320°C.

The result of the fibroin, when compared to that of sericin, showed the same TG scan and DTA thermograms up to 300°C. A clear endothermic peak appeared on the DTA thermogram of the β -type fibroin⁹ resulting in the onset of decomposition of fibroin molecules at 310°C. Moreover, maximum decrease of the fibroin (β -type) weight occurred at about 300°C (Fig. 3).

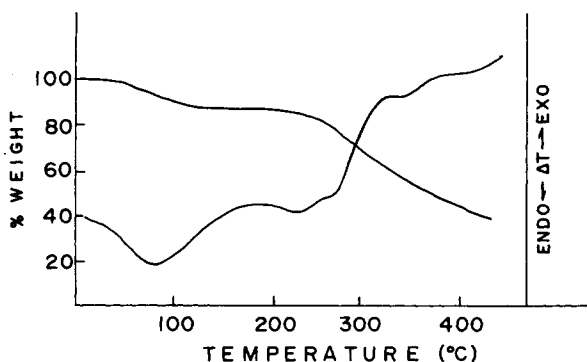


Fig. 2. DTA and thermogravimetry thermograms of Nd-s/Nd-s sericin cocoons.

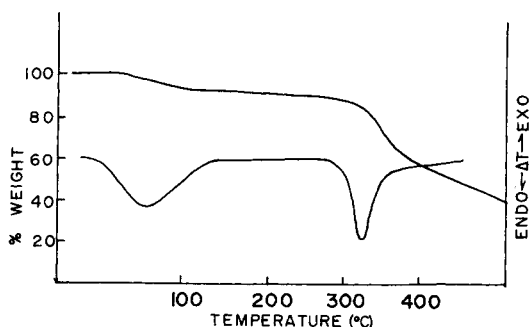


Fig. 3. DTA and thermogravimetry thermograms of β -type fibroin.

DTA curves (Fig. 4) of sericin cocoons (Nd-s/Nd-s, Nd-s/+) show more distinct and significant endothermic peaks than those peaks of the fibroin and the sericin stripped from the silk gland. The first and second endothermic peaks are due to the normal volatilization of absorbed water⁹ in the samples. The second endothermic peak of the sericin gradually occurs from 170°C upward, and shows its maximum at around 220°C.

A distinct endothermic peak (the fourth peak) of the Nd-s/Nd-s and Nd-s/+ sericin cocoons occurs at 310°C more clearly than that of the Nd and the sericin stripped from the silk gland removed from the matured silkworm, while Nd and sericin stripped from the silk gland show a slightly small shoulder at the same temperature. The DTA thermograms of degummed fibroin (β -type) show a distinct thermal decomposition peak at 315°C, while coagulated fibroin shows a broad endothermic peak at 280°C. This difference in endothermic temperature of α - and β -fibroin can be explained as follows: While oriented and crystallized β -fibroin displays an endothermic peak at 310°C, the coagulated fibroin (x-ray diffraction of α -structure) has an α - β transition temperature at 240°–250°C, and the resulting β -type fibroin displays a characteristic endotherm re-

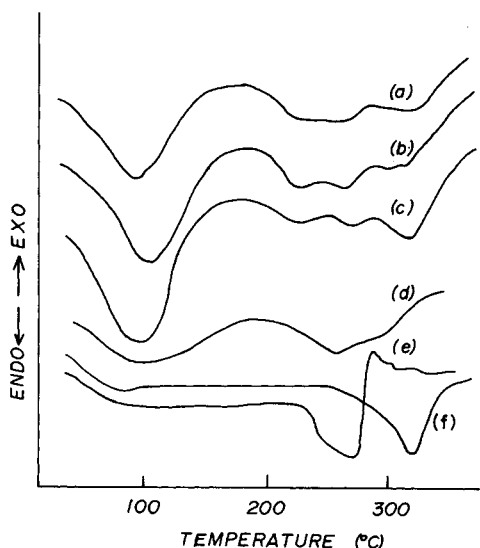


Fig. 4. Micro-DTA thermograms of sericin and fibroin: (a) Nd-s/Nd-s; (b) Nd; (c) Nd-s/+; (d) sericin stripped from silk gland; (e) coagulated fibroin; (f) β -type fibroin.

action associated with decomposition at 280°C. Our previous report^{8,9} has already clarified these thermal characteristics of the silk fibroin in connection with the decomposition behavior by analyzing the DSC thermograms.

The amount of fibroin messenger-RNA in the posterior silk gland of normal and mutant *Bombyx mori* has been measured and quantitatively detected by Suzuki.⁷ It showed that Nd-s/+ sericin has 15 μg (amount in a pair of posterior silk glands) fibroin messenger-RNA, and this measured amount is 10 times more than that in the other sericin cocoons (Nd, 1.4 μg ; Nd-s/Nd-s, 1.3 μg). Moreover, it is generally noted that the Nd-s/+ sericin cocoon layer has more silk fibroin substance than other types of sericin cocoons. From the above data, the fourth endotherm peak which appeared on the micro-DTA thermogram at about 320°C probably occurred through partially oriented β -type fibroin decomposition. This partial orientation of the fibroin seems to be caused by shear forces between the excretory division, which is the spinning organ, and the liquid silk fibroin molecules.

On the other hand, sericin stripped from coagulated silk fibroin relates to the endothermic peaks appearing on the DTA thermogram, but sericin which is stripped from the silk gland only shows the third peak around 262°C. According to the above TG measurement of sericin, a significant decrease in weight is clearly noted at 220°C on a DTA profile, and at the same time an endothermic reaction occurs on the DTA thermograms.

From the thermal analysis results of the sericin cocoon (Nd-s/Nd-s), the second endothermal peak at 220°C is considered to be a product of the molecular scission and the flowing of the sericin molecule, followed by a decomposition reaction. This was also confirmed^{6,10} by viscoelasticity measurements ($\tan\delta$) and the thermomechanical analysis of the sericin cocoon.

Aoki et al.⁵ reported the thermal behavior of Nd sericin cocoon and classified sericin using the Mosher method based on the solubility difference of the sericin in hot water.³ According to Aoki, the Mosher sericin A and B also show the second and third endotherm peak in the DTA profile; but in this experiment, the sericins, which are stripped from the coagulated fibroin and sericin (1, 2, and 3), classified by Shimizu, show different results in the DTA measurement.

To investigate these differences, sericins 1, 2, and 3 were subjected to DSC analysis (Fig. 5). In these thermograms, each sericin indicates a distinct endothermal peak at 221°, 225°, and 226.5°C, and these peaks correspond closely with the second peak on the DTA profile of sericin cocoon. On the other hand, the classified sericins, extracted by boiling water, do not show the third endothermal peak. The slight shift to higher temperature of the endothermal peak of these sericins (1, 2, and 3) may be related to differences in crystallinity.

The density measured by the density gradient column method for sericin summarizes as follows; sericin 1, 1.386; sericin 2, 1.389; sericin 3, 1.394. The crystallinity of the sericin measured by Komatsu¹² for sericins 1, 2, and 3 agrees with these experimental results.

Measurement of Color Changes

Color change of sericin cocoon (Nd-s/Nd-s) is visually recognized by heating. (Changes are from white to light yellow, deep yellow, light brown, and black). These appreciable changes resulting from heat occur at around 190°C, but it has

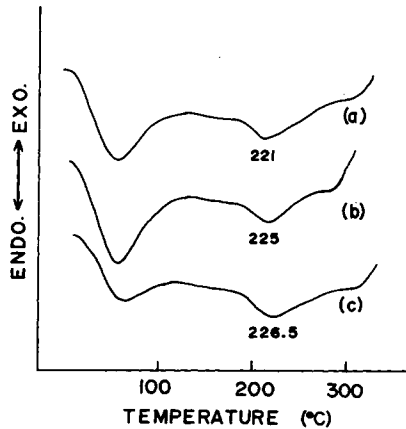


Fig. 5. DSC thermograms of sericin 1 (a), sericin 2 (b), and sericin 3 (c) extracted from the cocoon layer (*Bombyx mori*) by boiling water after the method of Shimizu.

been very difficult to relate quantitative changes corresponding to these color changes. The author has achieved this objective by measuring the physical quantity L/b by the color difference meter, where L denotes lightness and b denotes yellowness. Values were obtained as digital figures.

From the results of the color measurement (L/b) of the sericin cocoon attained by heating (Fig. 6), appreciable and remarkable changes are recognized at the temperature interval from 170° to 210°C. The physical quantity L/b should decrease when the sericin surface color changes by heating from white to brown or black because of decreasing lightness (L) and increasing yellowness (b). Since the temperature at which its color changes coincides with that of the endothermic reaction temperature (220°C) L/b could be expressed as an index corresponding to the scission and flowing of sericin molecules.

X-Ray Diffraction Pattern

Figure 7 shows the x-ray diffraction patterns of the sericin (Nd-s/+) heated to the required temperature in the DTA furnace. We recognize that the strongest diffraction, which corresponds to 4.54 Å, from the solid sericin cocoon begins to

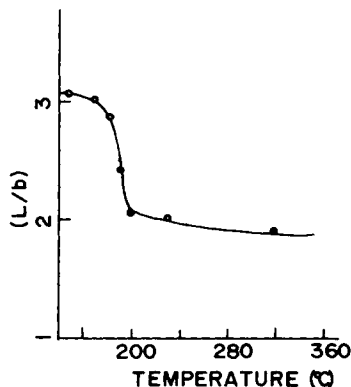


Fig. 6. Color change index L/b of Nd-s/Nd-s sericin cocoons measured by color difference meter: L , whiteness; b , yellowness.

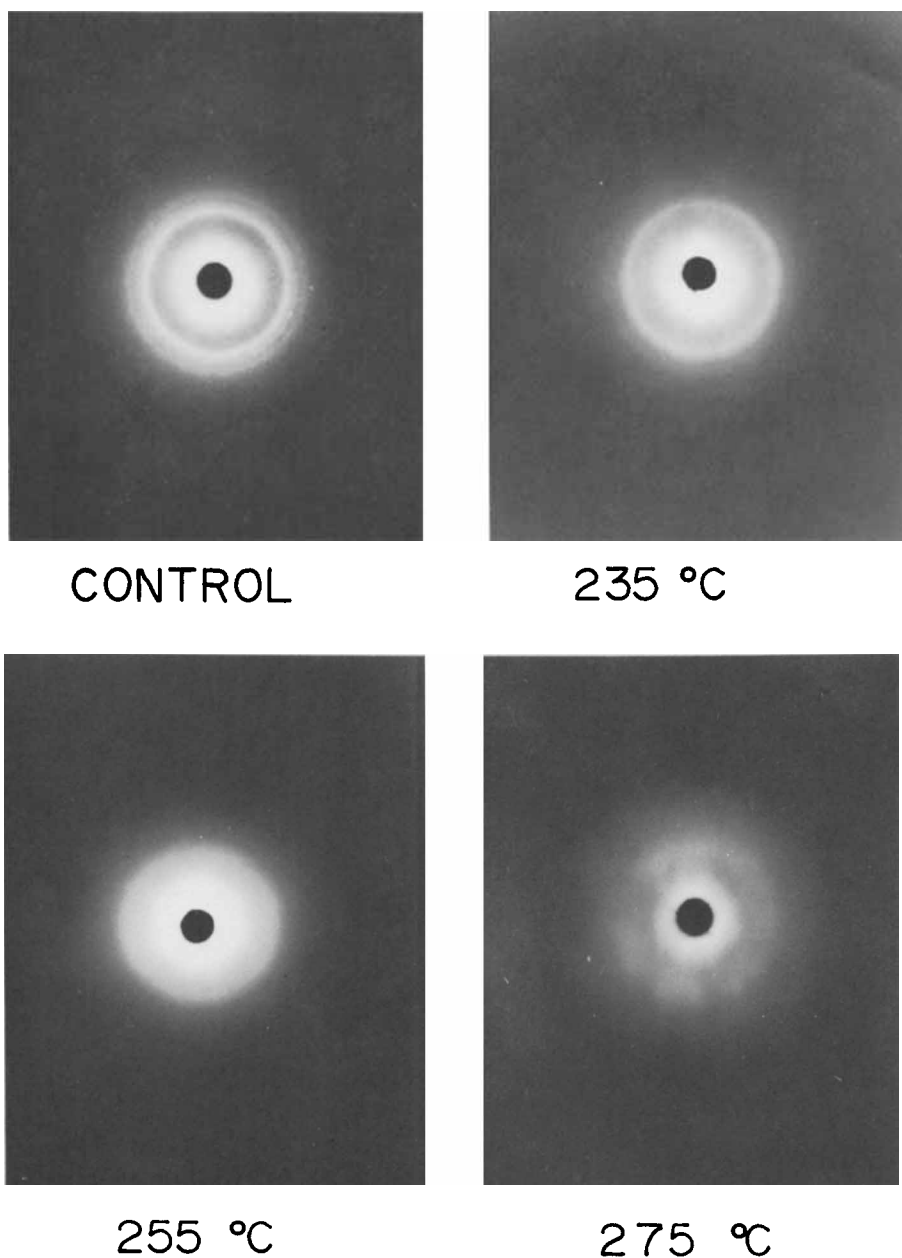


Fig. 7. X-Ray diffraction pattern of sericin (Nd-s/+) cocoon heated to required temperature in the DTA furnace.

disappear at temperatures above 270°C. This temperature corresponds to the third endothermic temperature shown on the DTA thermograms for Nd-s/+ sericin cocoon where the amorphous structure begins to appear. This critical temperature for the sericin cocoon (Nd-s/Nd-s, Nd, Nd-s/+, and Pnd, and stripped sericin from the silk gland) also coincides with the temperature for the third endothermic peaks on the DTA thermogram (Table I). These results agree well with the thermal analysis and IR measurements by Aoki and Takeuchi in

	D T A				E G D			
	1st	2nd	3rd	4th	1st	2nd	3rd	4th
Nd-s/Nd	83	220	270	320 _s	80	—	272	310
Nd	78	227	270	320 _s	80	—	275	316
Nd-s/+	80	227	272	322	75	—	295	320
stp. ser.	83	—	263	—	80 _s	—	250	318
coag. fib			289				287	

which they used the Nd sericin as sample. As mentioned above, the second, third, and fourth endothermic peaks of the DTA thermogram of the sericin (Fig. 3) can be considered closely connected to molecular flowing and scission, transition from crystalline to amorphous structure, and degradation or disintegration of partly contaminated fibroin in the sericin cocoon.

Evolved Gas Analysis and Evolved Gas Detection

If scission of the sericin molecule occurs, gas may be evolved from sericin cocoon and fibroin. Figure 8 shows the EGA results of the sericin cocoons (Nd, Nd-s/Nd-s, and Nd-s/+, and sericin stripped from the silk glands) and fibroin (coagulated fibroin and β -type fibroin¹¹). Gas evolved from sericin cocoon

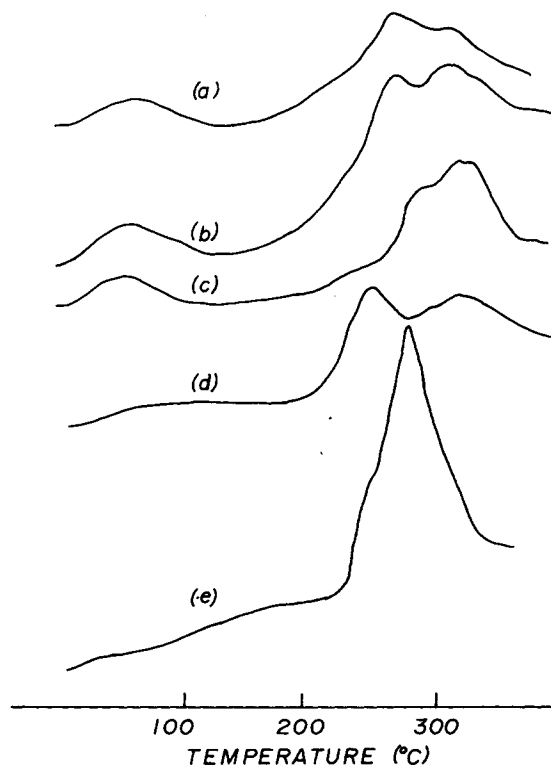


Fig. 8. Thermally evolved gas detection curves of sericin cocoons and fibroin: (a) Nd-s/Nd-s; (b) Nd; (c) Nd-s/+; (d) sericin stripped from silk gland; (e) coagulated fibroin.

presents a great contrast to that of fibroin (α -type) (Fig. 8). In the thermograms, from an onset temperature of about 30°C to a temperature approaching 160°C, the evolved gas analysis curves of sericin show that the initial reaction and its maximum EGD peak occur at about 80°C. The EGD curves return to the baseline by 160°C. This peak occurs for the same reasons discussed in the preceding consideration of the DTA thermograms. From an onset temperature of around 160°C, slight gas evolution is detected, and the analysis of evolved gas from sericin cocoon and coagulated fibroin have their inflection points at about 180° and 240°C, respectively. From these temperatures, the evolved gas detection curves show a slight increase in gas evolved from sericin cocoon.

The temperature of the EGA peak closely corresponds to the endothermic peak displayed in the DTA thermograms (Table I). For example, the temperature of the endothermal peaks appearing on the DTA thermograms of Nd-s/+ sericin cocoons (80°, 295°, and 322°C) correspond well to the peak temperatures which occur on the EGA curves (75°, 295°, and 320°C). The fourth peak of Nd-s/Nd-s and Nd sericin cocoons is not sharp. The second peak appearing on the DTA curves does not occur on the EGD curves. On the other hand, the EGA curve of fibroin (α -type) displays only a single peak at 287°C.

By using gas-chromatographic analysis in which the volatilization gas from the sericin and fibroin was heated up to various stages, the gases from the samples could not be identified.

Detection of the gas from the sericin cocoon can be identified using the parallel separation method (Figs. 1 and 9). Parts (A), (B), and (C) of Figure 9 are the results of 55°, 275°, and 348°C, respectively. Peaks a, b, c, d, and e correspond to O₂, N₂, CH₄, CO₂, and CO. According to these results, while O₂, N₂, CH₄, and CO do not change noticeably with increase in temperature, noticeable changes in the amount of CO₂ can be seen. Judging from the structural characteristics of these samples, it cannot be considered that O₂ and N₂ gas were thermally volatilized from the silk substance but arise from the contamination of the air entering the measuring column when the cock is switched over to stock the evolved gas.

The detection of CO₂ gas seems to depend on the evolving temperature. The quantitative amount of CO₂ was measured, and the results are shown in Figure 10. This detection was carried out only for the quantitative analysis of CO₂ evolved from the sericin cocoon. The dimensional unit of the detection of CO₂

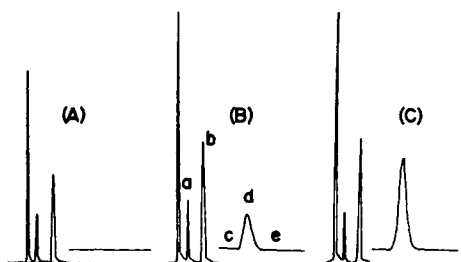


Fig. 9. Results of evolved gas analysis from Nd-s/Nd-s sericin cocoon schematically shown: (A), (B), and (C) are results at 55°, 275°, and 348°C, respectively. Peaks of a, b, c, d, and e correspond to the gases O₂, N₂, CH₄, and CO.

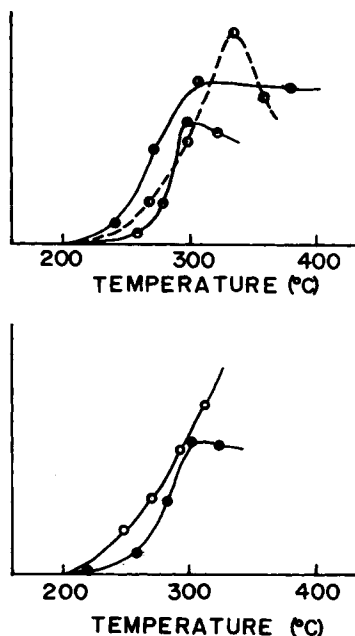
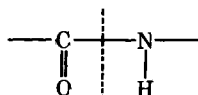


Fig. 10. Thermal evolved gas (CO₂) per sample weight from sericin cocoons and fibroin. The dimensional unit corresponding to CO₂ evolved from the sample is omitted because of the quantitative analysis.

is omitted in Figure 10. CO₂ slowly begins to evolve from the sericin cocoon at about 200°C, and CO₂ EGA curves have inflection points at around 270°C. Nd-s/+ and sericin stripped from the silk gland have a CO₂ EGA Peak at 300°C, but the EGA peak of Nd-s/Nd-s sericin cocoon reaches a higher temperature (325°C). From Figure 10 it is also observed that CO₂ from the Nd sericin cocoon reaches a constant and will not increase any more even if the temperature increases. On the other hand, CO₂ gas from the coagulated fibroin begins gradually to evolve from 200°C in the form of an increasing curve.

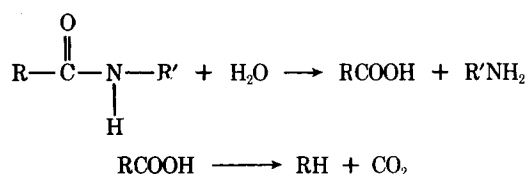
In carrying out the mass-spectrographic analysis of a polyamide, Achamer and Straus¹³ have inferred that the scission of the amide molecule occurs at the weakest part of the amide molecule bond:



This scission gives rise to an accompanying reaction which produces a certain amount of CO₂ and H₂O. If there should be a small amount of water generated in the sample, the water hydrolyzes the amide bond of the silk substances (sericin, fibroin) and brings about decarboxylation, which produces CO₂.

The author has adopted this concept as a working hypothesis for proteins. The CO₂ gas evolved from the thermal degradation of sericin and fibroin has been identified as the by-product gas. CO₂ evolution from the sericin cocoon can be explained assuming that decarboxylation of the peptide bond is induced after

the dehydration of part of the molecule:



In the TG thermograms of the sericin, the maximum decrease in weight occurs at 220°C; but on the EGA curves, a maximum peak occurs at 300°C. This difference in peak temperature (80°C) arises for the following reason: In the TG scan, the maximum peak occurs at the inflection points of the DTA scanning curve, and evolved gas from the sample can be detected in the EGA curves. If this reasoning is correct, the maximum peak of fibroin and sericin in EGA measuring should occur at a specific temperature. The detected amount of CO₂ gas from the coagulated fibroin can be seen as an increasing curve below 310°C. Therefore, we can estimate that the peak which corresponds to a decrease in the weight of the sample would occur at 300°C.

Appendix

Silk is an extracellular fiber extruded by the silkworm from a pair of glands. The gland is large and tubular and folds upon itself posteriorly. The silk gland is divided into anterior, middle, and posterior sections (Figs. 11 and 12). The silk thread is in the form of a double filament of the protein fibroin, enveloped in an outer coating of silk glue, or sericin, which acts as an adhesive. The main fibroin component of silk fibroin is produced in the posterior division of the gland, while the gelatinous component, sericin, is secreted in the middle division (Fig. 12).

The different gene types of silkworms used in this experiment are Nd-s/Nd-s, Nd-s/+, and Nd.

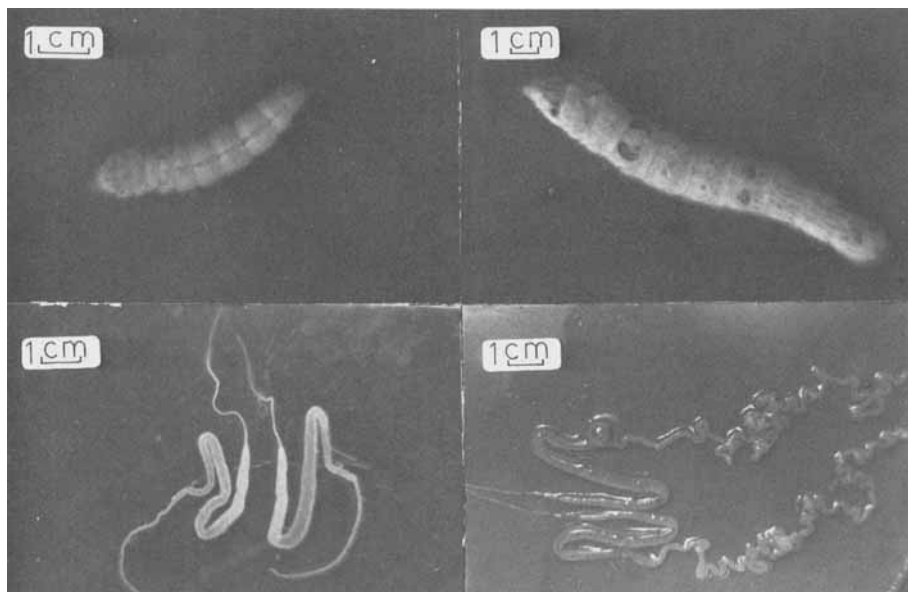


Fig. 11. Outstanding differences between homozygote (Nd-s/Nd-s) and heterozygote (Nd-s/+) silkworms.

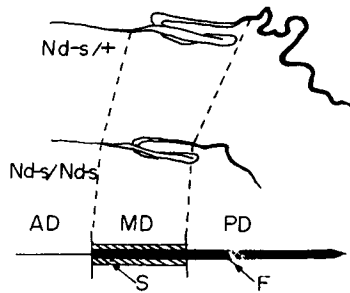


Fig. 12. Schematic diagram of homozygote (gene symbol $Nd-s/Nd-s$) and heterozygote (gene symbol $Nd-s/+$) silk glands: AD, anterior division; MD, middle division; PD, posterior division; S, sericin; F, fibroin.

The gene symbol $Nd-s^{15}$ represents the sericin cocoon whose filament contains only sericin; gene symbol Nd^{16} means naked (gene name). $Nd-s/Nd-s$ is the gene symbol of the homozygote silkworm, while $Nd-s/+$ is the gene symbol of the heterozygote silkworm. Figure 12 shows, for example, the outstanding differences of homozygote and heterozygote silkworms. Posterior divisions of the homozygote silkworm degenerate into thin and small organs, which means that the layers of the homozygote silkworm cocoons contain less sericin.

The author wishes to express his appreciation to Dr. Konda and Dr. Ishikawa, Faculty of Textile Science and Technology, Shinshu University, and to Dr. Hirabayashi, Faculty of Technology, Tokyo University of Agriculture and Technology, for their helpful discussions. The author also thanks Dr. Gamo and Mr. Yasumura of the Sericultural Experimental Station for their generous supply of sericin cocoons, and Dr. Samuel Gilberg and Mrs. Laurie Vander Velde for critical reading of the manuscript.

References

1. H. A. Rutherford and M. Harris, *Am. Dyest. Rep.*, **29**, 213 (1940).
2. M. Simizu, *Bull. Imp. Sericult. Exp. Sta. Jpn.*, **10**, 441 (1941).
3. H. H. Mosher, *Am. Dyest. Rep.*, **21**, 241 (1932).
4. N. Koide, *Sen-i Gakkaishi (J. Soc., Fiber Sci. Tech. Jpn.)*, **26**, 53 (1970).
5. I. Aoki and T. Takeuchi, *Sen-i Gakkaishi*, **27**, 486 (1971).
6. K. Hirabayashi, M. Tsukada, H. Ishikawa, and S. Yasumura, *Sen-i Gakkaishi*, **30**, T-459 (1974).
7. Y. Suzuki and E. Suzuki, *J. Mol. Biol.*, **88**, 393 (1974).
8. K. Hirabayashi, M. Tsukada, M. Nagura, and H. Ishikawa, *Sen-i Gakkaishi*, **31**, T-8 (1975).
9. H. Ishikawa, M. Tsukada, I. Toizume, A. Konda, and K. Hirabayashi, *Sen-i Gakkaishi*, **28**, 91 (1972).
10. K. Hirabayashi, M. Tsukada, S. Seiji, H. Ishikawa and S. Yasumura, *J. Sericult. Sci. Jpn.*, **41**, 349 (1972).
11. T. Sugaya and T. Owawa, *Sericult. Res. Commun.* **24**, 132 (1974).
12. K. Komatsu, *Bull. Imp. Sericult. Exp. Sta. Jpn.*, **26**, 136 (1975).
13. M. B. Neiman, *Aging and Stabilization of Polymers*, Sangyo Tosho Co., Ltd. (translated by Inaba and Iiyama), . . . , p. 206. Tokyo, 1966.
14. T. Gamo, *Jpn. J. Genet.*, **48** (No. 2), 99 (1973).
15. Y. Nakano, *J. Sericult. Sci. Jpn.*, **20**, 232 (1951).
16. Y. Horiuchi, C. Namishima, K. Nakamura, and N. Yasue, *J. Sericult. Sci. Jpn.*, **32**, 195 (1963).

Received July 29, 1976

Revised January 10, 1977